International Journal of Impact Engineering 37 (2010) 82–89

Contents lists available at ScienceDirect

International Journal of Impact Engineering

journal homepage: www.elsevier.com/locate/ijimpeng

Experimental investigation of response of monolithic and bilayer plates to impulsive loads

M.R. Amini, J.B. Isaacs, S. Nemat-Nasser*

Center of Excellence for Advanced Materials, Department of Mechanical and Aerospace Engineering, University of California, San Diego, La Jolla, CA 92093-0416, USA

ARTICLE INFO

Article history:
Received 6 August 2007
Received in revised form
8 April 2009
Accepted 13 April 2009
Available online 22 April 2009

Keywords:
Blast protection
Fluid–structure interaction
Metal–elastomer bilayer plate
Experimental fracture analysis

ABSTRACT

This article presents the results of a series of experiments performed to assess the dynamic response of circular monolithic steel and steel–polyurea bilayer plates to impulsive loads. A convenient technique to enhance the energy absorption capability of steel plates and to improve their resistance to fracturing in dynamic events, is to spray-cast a layer of polyurea onto the plates. Since polyurea readily adheres to metallic surfaces and has a short curing time, the technique may be used to retrofit existing metallic structures to improve their blast resistance. We have examined the effectiveness of this approach, focusing on the question of the significance of the relative position of the polyurea layer with respect to the loading direction; *i.e.*, we have explored whether the polyurea layer cast on the *front face* (the impulse-receiving face) or on the *back face* of the steel plate would provide a more effective blast mitigating composite.

The experimental results suggest that the polyurea layer can have a significant effect on the response of the steel plate to dynamic impulsive loads, both in terms of failure mitigation and energy absorption, if it is deposited on the *back face* of the plate. And, remarkably, when polyurea is placed on the *front face* of the plate, it may actually enhance the destructive effect of the blast, promoting (rather than mitigating) the failure of the steel plate, depending on the interface bonding strength between the polyurea and steel layers. These experimental results are supported by our computational simulations of the entire experiment, employing realistic physics-based constitutive models for the steel (DH-36, in the present work) and polyurea [Amini MR, Amirkhizi AV, Nemat-Nasser S. Numerical modeling of response of monolithic and bilayer plates to impulsive loads. Int J Impact Eng, submitted for publication].

1. Introduction

In the past several decades, many researchers have investigated the dynamic deformation and failure modes of plates of various geometries and boundary conditions, under dynamic loads. Most of these studies have focused mainly on theoretical predictions, since the corresponding experiments are difficult to conduct. Also, for the experimental investigations, different experimental techniques and test conditions have been used that make the comparison of the results difficult. Nurick and Martin [2] have compared the different experimental techniques used to study the dynamic deformation and failure of the plates. These experiments include: pressure waves created by explosive devices; under-water explosion; and direct impulse using plastic sheet explosives. More recently, Radford et al. [3] studied the dynamic deformation of plates using an experiment based on direct impact by metal-foam projectiles.

The existing experimental investigations [4–7] have led the researchers to define three failure modes (referred to as Modes I, II, and III), for beams and plates subjected to impulsive loads. These are:

Mode I – large inelastic deformation
Mode II – tensile tearing at the edges
Mode III – shear failure at the edges.

In this study, a new reverse ballistic technique has been developed and successfully implemented at UCSD's Center of Excellence for Advanced Materials (CEAM). Using this method, one can apply a controlled dynamic pressure load on a plate, record its deformation and possible fracturing by high-speed photography, and hence be able to compare, both quantitatively and qualitatively, the resulting sample response under various reproducible conditions. The reverse ballistic tests on plates were performed at

* Corresponding author.
E-mail address: sia@ucsd.edu (S. Nemat-Nasser).

0734-743X/$ – see front matter © 2009 Elsevier Ltd. All rights reserved.
doi:10.1016/j.ijimpeng.2009.04.002

CEAM/UCSD's gas gun facilities laboratory. In this study, a projectile, carrying a plate, is propelled by a gas gun at a controlled velocity towards a soft polyurethane target that rests against a 76.2-mm Hopkinson bar within a confining steel cylinder. Soft polyurethane with a durometer hardness of 40 A is used to load the plate. Two types of plates are studied: monolithic DH-36 steel plates and steel–polyurea bilayer plates. Each bilayer plate consists of a polyurea layer spray-cast onto a DH-36 steel plate. Fig. 1 is a schematic view of the reverse ballistic experimental setup. The main goals of this study are:

(i) To investigate the dynamic response and fracture of monolithic steel plates under impulsive loads, with the aim of exploring the underpinning mechanisms of the deformation and the failure modes.
(ii) To demonstrate the effect of the polyurea coating on the dynamic response and fracture of steel plates under impulsive loads, focusing on the significance of the relative position of the polyurea layer with respect to the loading direction.
(iii) To use the experimental results to investigate the accuracy of the finite-element modeling and the prediction of the dynamic response and fracture of steel plates with and without polyurea coating; see [1] for numerical simulations, analysis, and the discussion of the results.

The reverse ballistic experiment is designed such that the failure of the plates occurs near their center, involving deformation localization and necking at the central region of the plate accompanied by radial and circumferential crack propagation and possible petaling and disking.

Polyurea at room temperature is highly elastic, flexible, and resistant to abrasion, impact, and weather. This elastomer has been extensively used in the coating industry in solid form. Its growing acceptance derives in part from the ease with which this material can be spray-cast onto retrofit steel plates, and in part because of its excellent performance in otherwise normally corrosive environments. Recent studies [1,8,9] show that applying a layer of polyurea (thickness of 1–3 mm) to steel plates (of thickness 1 mm) can vastly improve their ballistic efficiency. Mock and Balizer [10] experimentally observed that the polyurea coating can change the response of the steel plate from full penetration of a ballistic projectile to complete mitigation of its fracture.

In this study, a reverse ballistic technique is employed to explore the effect of the polyurea coating on the dynamic response and failure of simply supported circular steel plates, focusing on the question of the significance of the relative position of the polyurea layer with respect to the loading direction, *i.e.*, whether the polyurea cast onto the *front face* or onto the *back face* of the steel plates would provide better blast mitigating composites. In addition, the experimental results revealed that the initial kinetic energy per unit thickness of the steel layer is a reasonable parameter to quantify the experimental results.

First the experimental procedure and the material used to fabricate the samples are discussed. Then the experimental observations and results are reported and discussed.

2. Materials, samples, and experiments

Monolithic plates are made from DH-36 steel, a high strength structural steel used in naval applications. This steel has high toughness and high strength under various load and temperature conditions. Its mechanical properties have been systematically studied over a broad range of strain rates (from 0.001/s to about 8000/s) and temperatures (from 77 to 1000 K) by Nemat-Nasser and Guo [11] who also developed a physics-based (PB) constitutive model for the material. Since the mechanical characteristics of the DH-36 steel plates may vary depending on the rolling and other factors, we have checked the high strain-rate stress–strain relations for the present case and compared the results with those reported in [11], observing that the plate used in the current study has about 10% higher flow stress compared with the one considered by Nemat-Nasser and Guo [11]. The adjustment to the model parameters was however quite minor, as is explained in [1]. This model has thus been incorporated into the finite-element code, LS-DYNA, and used to predict the experimental results.

The composite plate consists of a polyurea layer directly cast onto the steel plate. The physical properties of polyurea vary with its composition. The specific polyurea used in the present work is based on Isonate 2143L [12] and Versalink P1000 [13]. A five percent excess of Isonate 2143L is used to produce a lightly cross-linked polymer [14]. The glass transition temperature, T_g, is below $-50\ ^{\circ}C$ [14,15] which is well below the typical range of the service temperature. Above the glass transition temperature, polyurea has a nearly-elastic volumetric response and a viscoelastic shear response at moderate pressures and strain rates. The viscoelastic properties of this polyurea have been systematically studied by Amirkhizi et al. [16] over a broad range of strain rates and temperatures, including the high-pressure effects. Based on this, a pressure, temperature, and strain-rate sensitive model has been developed by these authors and implemented into LS-DYNA. The model involves only a finite number of internal variables and is specifically well-suited for use in an explicit finite-element code.

The monolithic plates are hand-machined from a 4.77 mm thick DH-36 steel sheet. Each steel sample is circular with a diameter of 76 mm, having a 4.77 mm thick rim of 57 mm inner diameter. The inner portion of the sample is about 1 mm thick; see Fig. 2. The dimensions of each plate are measured at various locations and averaged to arrive at a nominal value. The thickness of the plates varies from 0.95 mm to 1.07 mm. In addition, the plates are weighed before each experiment.

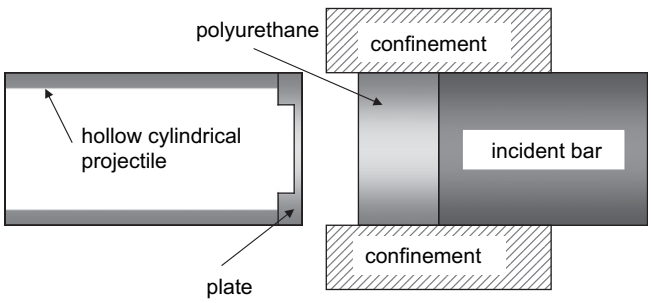

Fig. 1. Schematic view of the reverse ballistic experimental setup.

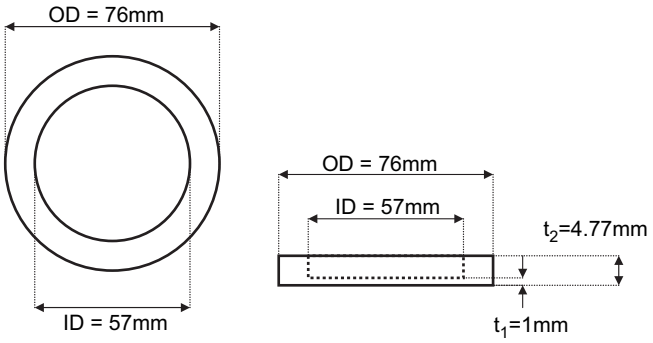

Fig. 2. Schematic view of monolithic steel plate: geometry and dimensions.

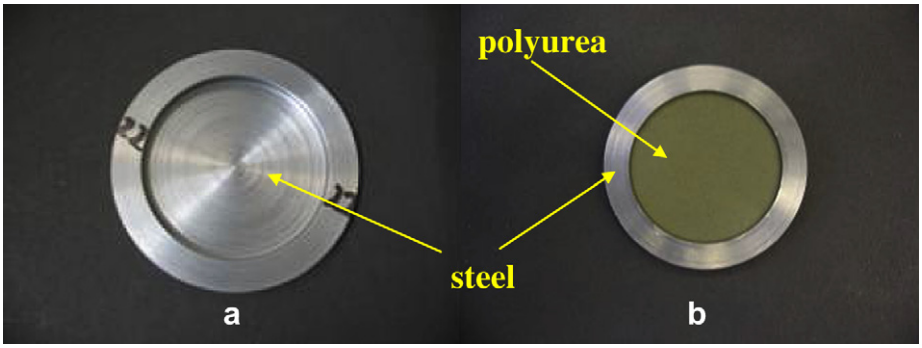

Fig. 3. Un-deformed steel plates: (a) without polyurea coating (left side); (b) with polyurea coating (right side).

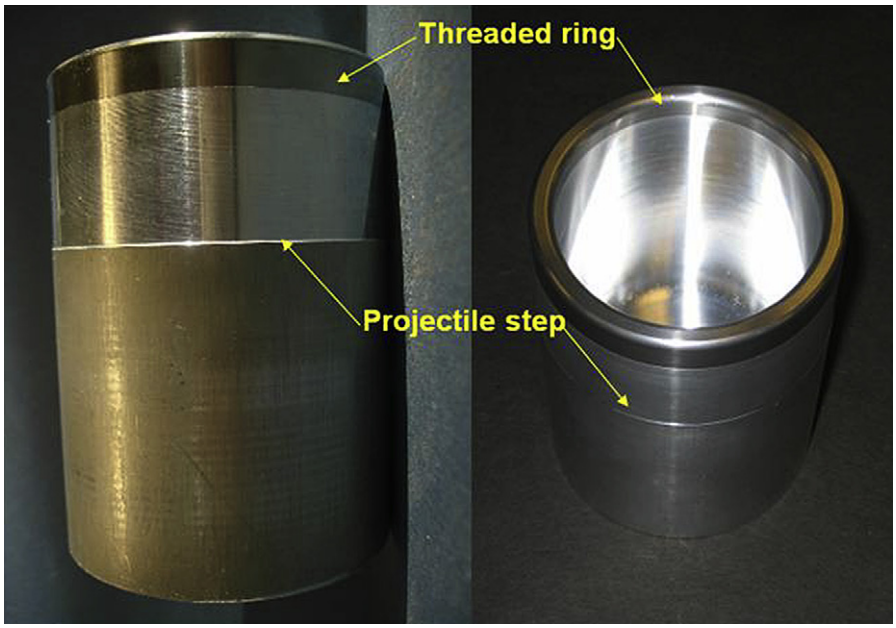

Fig. 4. Projectile used in *set-II* experiments, comprised of a stepped 7075 aluminum tube and a threaded steel ring (left: side view; right: angled view).

The polyurea layer of the bilayer plates is cast onto the inner portion of the sample and hence is about 3.77 mm thick. In a typical test, the plate (monolithic or bilayer) impacts a 25.4 mm thick soft polyurethane layer of 40 A durometer hardness that rests against a 76.2-mm Hopkinson bar inside a confining steel cylinder, as shown in Fig. 1.The post-experiment visual inspection of the confining steel cylinder shows no permanent damage or plastic deformation of the confining steel. For the bilayer plates, the average thickness of each is also measured before and after the polyurea coating. The thickness of the polyurea layer is about 3.77 mm. Fig. 3 shows a typical un-deformed monolithic and a bilayer plate.

Two sets (denoted as *set-I* and *set-II*) of experiments are performed. In *set-I*, the projectile that carries the sample which impacts the polyurethane target is a 7075 aluminum cylindrical tube of 76.2 mm outer and 63.5 mm inner diameter, and 114.5 mm length. Since aluminum is a relatively soft metal, re-machining is required after each experiment. To avoid this, in the second set of tests (*set-II*), a 6.3 mm thickness, 76.2 mm outer and 63.5 mm inner diameter steel ring was threaded onto the projectile to protect the aluminum tube from damage; see Fig. 4. In this case, the sample sits on the steel ring, as it is carried by the projectile at a controlled velocity towards the polyurethane target. The properties of the materials used in this experimental setup are presented in Table 1.

Set-II experiments are subdivided into two subgroups, *set-IIA* and *set-IIB*, the first set being loaded on their flat side whereas the second being loaded on their dish side (with or without polyurea). The projectile, carrying the steel plate, is propelled by a gas gun at a controlled velocity, which is measured using velocity sensors placed at the end of the gas gun muzzle. Upon impact, the confined soft polyurethane loads the plate within a short interval (about several hundred microseconds). The steel plate deforms by stretching and bending that may result in localized deformation, necking, and fracture of the plate. The experiment is designed such as to simplify the modeling of its support against the cylindrical projectile as well as to ensure that the fracture and failure initiate within the central region of the steel plate.

Table 1
Material properties of the reverse ballistic experimental components.

Material/part	Density (kg/m^3)	Young's modulus (GPa)	Poisson ratio
7075 Aluminum/projectile	2770	70	0.345
Steel/output bar	7830	210	0.29
Steel/confinement	7830	210	0.29

Table 2
Experimental condition of first set of reverse ballistic tests: *set-I*.

Specimen					Projectile	Initial conditions	
Test	Plate type	Loading direction	Thickness (mm)	Mass (g)	Mass (g)	Velocity (m/s)	Kinetic energy (J)
S-8	Monolithic	Flat side	1.041	94.5	632.9	68.9	1727
S-9	Monolithic	Flat side	1.006	93.4	626.7	73.2	1929
S-10	Monolithic	Flat side	0.978	93.1	620.4	74.8	1996
S-11	Monolithic	Flat side	0.940	92.5	613.7	70.1	1735
S-12	Monolithic	Flat side	1.021	94.1	606.2	72.3	1830
S-13	Monolithic	Flat side	1.011	94.2	598.9	72.4	1817

The experimental conditions are summarized in Tables 2 and 3. The projectile velocities range from 64.9 m/s to 76.7 m/s, providing projectile kinetic energies of 1597–2234 J. Fig. 5 shows the experimental setup and its various components.

3. Results and analysis

A total of 30 tests are performed. Selected deformed plates are sectioned after the test and their final thickness and other dimensions are measured, from which the principal stretches can be calculated [1]. In addition, all the deformed plates are carefully examined for any visible signs of failure. Based on their response, the deformed plates are subdivided into three categories: no failure, moderate failure, and severe failure. The plates in the first category did not have any cracks but multiple parallel necks were visible in the central region of some of them. These cracks are typically up to 2 cm long and few millimeters apart. The second category samples developed severe necking with crack initiation and minor petaling. And, finally, the last category samples had radial and circumferential cracks with petaling and possibly disking or edge tearing. A typical sample of each failure category is shown in Fig. 6.

3.1. Effect of plate thickness

The strength of the specimen increases if its thickness is increased. The membrane stiffness varies linearly with the plate thickness while the bending stiffness relates linearly to the square of the thickness. At low velocities, the deflection is small and hence the bending is dominant, while the stretching effect becomes significant at high impact velocities which produce large tensile deformation. In large deformations, the plastically dissipated work in the membrane deformation is much larger than that in the bending deformation. Therefore, the energy absorbed by the specimen's plastic deformation has a linear relation with the thickness at large deformations. This means that for the same impact velocity, as the thickness of the specimen increases, the kinetic energy that is converted into the plastic work increases linearly with the thickness. Therefore, kinetic energy per unit thickness of the steel layer may be used as a parameter to quantify the dynamic performance efficiency of this structure. It is experimentally verified that this parameter can be used to predict the failure onset of the plates. The experimental results suggest that when the impact kinetic energy per unit thickness is greater than an experimentally-obtained critical value, the sample fails. This critical value depends on the experimental conditions.

3.2. Deformation and failure mechanisms

In the monolithic steel-plate experiments, fracture seems to begin with the onset of necking. Deformation then localizes, giving rise to large local plastic strains within the neck region where cracks initiate and grow circumferentially near the center, and/or radially towards the edge of the plate, the actual crack path being affected by the imperfections and other statistical parameters. Multiple parallel necking patterns can be visually detected in the central region of some of the deformed samples.

Table 3
Experimental conditions of second set of reverse ballistic tests: *set-II*.

Specimen					Projectile	Initial conditions	
Test	Plate type	Loading direction	Thickness (mm)	Mass (g)	Mass (g)	Velocity (m/s)	Kinetic energy (J)
S-14	Monolithic	Flat side	0.998	89.5	657.4	72.0	1936
S-15	Monolithic	Flat side	0.998	90.3	657.4	71.5	1911
S-16	Monolithic	Flat side	1.001	88.4	657.4	71.6	1912
S-17	Monolithic	Flat side	0.975	89.5	657.2	72.0	1935
S-18	Monolithic	Flat side	1.002	90.3	657.2	71.7	1921
S-19	Monolithic	Flat side	0.996	90.6	657.2	71.7	1922
S-20	Monolithic	Flat side	0.966	89.6	657.2	73.5	2017
S-21	Monolithic	Flat side	0.977	90.0	657.2	73.6	2024
S-22	Monolithic	Flat side	0.978	90.2	657.2	73.4	2013
S-25	Monolithic	Flat side	0.995	91.1	657.2	73.6	2027
S-26	Monolithic	Flat side	1.009	91.5	656.1	72.1	1943
S-27	Monolithic	Flat side	0.988	90.3	656.1	72.5	1962
S-29	Monolithic	Flat side	1.014	91.7	656.1	76.4	2182
S-32	Monolithic	Flat side	0.992	91.1	656.1	74.7	2085
SP-41	Bilayer	Flat side	0.951	101.1	656.1	72.4	1985
SP-42	Bilayer	Flat side	1.064	106.8	656.1	72.2	1988
SP-44	Bilayer	Flat side	1.061	103.5	656.1	76.7	2234
S-45	Monolithic	Flat side	1.069	93.6	656.1	76.4	2188
S-28	Monolithic	Dish side	0.946	88.9	656.1	70.5	1851
S-31	Monolithic	Dish side	0.997	91.6	656.1	72.3	1954
SP-36	Bilayer	Dish side	0.991	102.3	656.1	64.9	1597
S-46	Monolithic	Dish side	1.046	94.7	656.1	67.0	1685
S-48	Monolithic	Dish side	1.029	94.3	656.1	67.7	1720
S-51	Monolithic	Dish side	1.065	95.2	656.1	67.3	1701

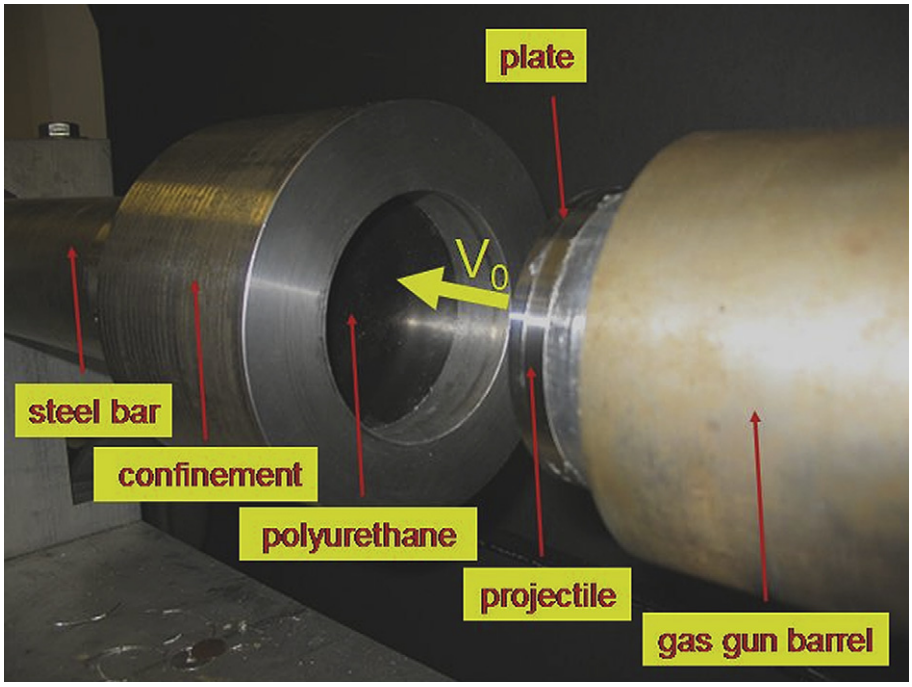

Fig. 5. Experimental setup. The projectile carrying the steel plate is propelled by a gas gun at a controlled velocity towards the confined polyurethane target that rests against a 3-inch steel bar.

3.3. Experimental results

The results of the two sets of experiments are summarized in Tables 4 and 5 and further discussed below. The main difference between the two test sets is the amount of energy that is dissipated through the rotation of the steel rim.

3.3.1. Set-I

Only monolithic plates are used in this set of experiments. The kinetic energy per unit thickness varies from 16,586 J/cm to 20,409 J/cm. The average rotation of the edge for this set of experiments is about 35°. The two samples with kinetic energy per unit thickness of less than 17,950 J/cm did not fail. On the other hand, the plate with kinetic energy per unit thickness of 20,409 J/cm (S-10) experienced severe failure.

3.3.2. Set-II

This set includes 24 tests that are divided into two groups: those loaded on the flat side (referred to as *set-IIA*) and those loaded on the dish side (referred to as *set-IIB*) of the steel plate, as indicated in

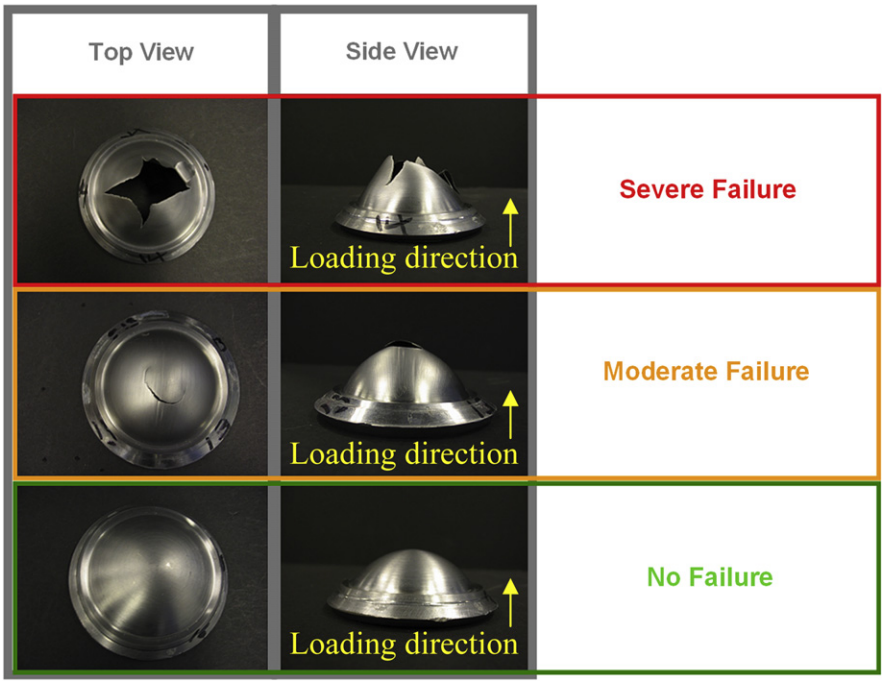

Fig. 6. Side view (right column) and top view (left column) of selected sample for each category of deformed steel plates: severely failed, moderately failed, and not failed.

Table 4
Summary of first set of reverse ballistic (*set-I*) experiments.

Specimen	Test condition		Result		
Test	Plate type	Loading direction	Initial kinetic energy per unit thickness (J/cm)	Edge rotation (°)	Failure
S-8	Monolithic	Flat side	16,586	35.0	N/A
S-9	Monolithic	Flat side	19,178	36.8	Moderate
S-10	Monolithic	Flat side	20,409	36.5	Severe
S-11	Monolithic	Flat side	18,459	32.8	Moderate
S-12	Monolithic	Flat side	17,927	36.0	N/A
S-13	Monolithic	Flat side	17,969	35.5	Moderate

the third column of Table 5. Four samples are with polyurea coating, three of which are loaded on the flat side and one on the dish side.

The kinetic energy per unit thickness of the *set-IIA* tests varies from 18,6886 J/cm to 21,523 J/cm. All monolithic samples failed when the kinetic energy per unit thickness exceeded 19,300 J/cm whereas two bilayer samples did not fail for kinetic energy per unit thickness of 18,688 J/cm (SP-42) and 21,059 J/cm (SP-44) respectively, when the polyurea coating was on the face opposite to the impact surface, indicating the effective role of polyurea backing on enhancing the energy absorption of the steel plate. However, the third bilayer plate (SP-41) severely necked without any petaling at a kinetic energy per unit thickness of 20,8683 J/cm, showing the onset of failure. The overall higher critical kinetic energy per unit thickness of the steel plate of this set compared to the first set of experiments is due to the extra energy dissipated in the plastic deformation of the rim. The rim deforms axi-symmetrically and its rotation is measured as the angle between the rim in the deformed and un-deformed states. The average rim rotation of the samples in this set is about 56°, 75% higher than the corresponding average value in *set-I*. On the other hand, the kinetic energy per unit thickness of *set-IIB* test samples that are loaded on the dish side varies from 15,976 J/cm to 19,601 J/cm, significantly lower than the typical corresponding values of *set-IIA*. This difference in the critical kinetic energy per unit thickness is considered to be due to the rim rotation of these samples, which is remarkably lower (approximately 3 times) than that of the *set-IIA* samples, being caused by the difference in the applied torque. The results of the *set-IIB* experiments reveal that the presence of polyurea coating in front of the steel plate cannot mitigate the failure. Sample SP-36 with polyurea coating on the front side failed severely at a kinetic energy per unit thickness of 16,117 J/cm, although its rim rotated significantly more than the monolithic samples in *set-IIB*.

3.4. Discussion

The experimental results show the significance of the relative position of the polyurea layer with respect to the loading direction. This may be explained by considering the initial shock effect. When polyurea is cast on the impact side, it is loaded in compression. Experimental study at CEAM/UCSD [16] has shown that polyurea is a highly pressure sensitive elastomer, with its stiffness increasing remarkably with increasing pressure. When the confined polyurea is loaded in compression, its stiffness can increase 10–20 fold, thereby attaining a better impedance match with the steel plate. Consequently, more energy is transferred to the plate. On the other hand, when polyurea is cast onto the opposite side of the impact (back side), the soft polyurethane loads the steel plate first and then a part of this energy is transferred to the polyurea, compressing it and thereby increasing its stiffness, and hence the amount of the energy that it captures and damps because of its viscoelasticity. Fig. 7 compares the response of two plates that are deformed under essentially the same kinetic energy per unit thickness (of approximately 21 kJ/cm) loaded on the flat side (*set-IIA*), one without polyurea and the other with polyurea on its back side. As the figure suggests, the monolithic steel plate failed severely whereas no visible sign of failure and necking were detected in the polyurea-

Table 5
Summary of second set of reverse ballistic (*set-II*) experiments.

Specimen	Test condition		Result		
Test	Plate type	Loading direction	Initial kinetic energy per unit thickness (J/cm)	Edge rotation (°)	Failure
S-14	Monolithic	Flat side	19,398	47.8	Severe
S-15	Monolithic	Flat side	19,150	51.8	N/A
S-16	Monolithic	Flat side	19,098	48.3	N/A
S-17	Monolithic	Flat side	19,851	50.3	Moderate
S-18	Monolithic	Flat side	19,176	56.0	N/A
S-19	Monolithic	Flat side	19,299	55.8	N/A
S-20	Monolithic	Flat side	20,882	55.8	Severe
S-21	Monolithic	Flat side	20,714	53.5	Severe
S-22	Monolithic	Flat side	20,586	45.9	Severe
S-25	Monolithic	Flat side	20,369	54.9	Moderate
S-26	Monolithic	Flat side	19,258	57.9	Severe
S-27	Monolithic	Flat side	19,855	58.8	Severe
S-29	Monolithic	Flat side	21,523	60.3	Moderate
S-32	Monolithic	Flat side	21,015	59.3	Severe
SP-41	Bilayer	Flat side	20,868	57.3	Moderate
SP-42	Bilayer	Flat side	18,688	57.3	N/A
SP-44	Bilayer	Flat side	21,059	66.3	N/A
S-45	Monolithic	Flat side	20,468	70.8	Severe
S-28	Monolithic	Dish side	19,571	21.6	Severe
S-31	Monolithic	Dish side	19,601	22.5	Severe
SP-36	Bilayer	Dish side	16,117	28.0	Severe
S-46	Monolithic	Dish side	16,111	22.0	Severe
S-48	Monolithic	Dish side	16,712	18.3	Severe
S-51	Monolithic	Dish side	15,976	28.0	Severe

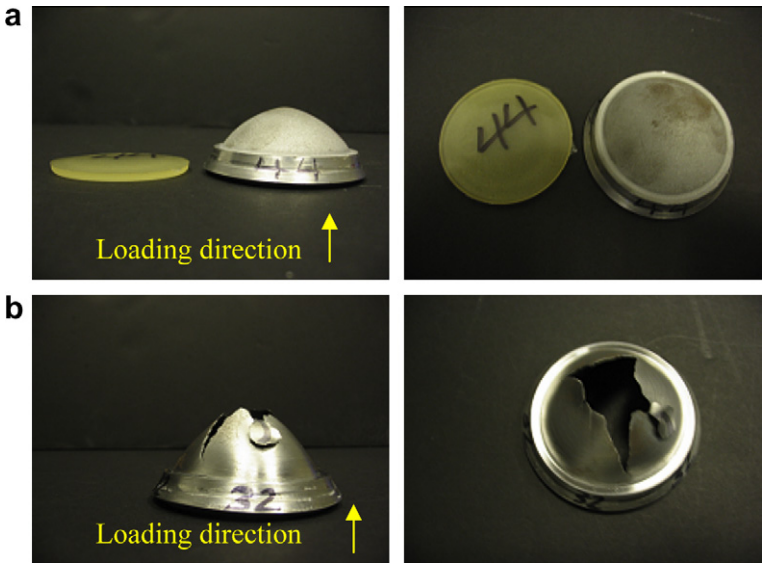

Fig. 7. Deformed steel-plate samples loaded on their flat side at approximately the same kinetic energy per unit thickness: (a) SP-44: bilayer plate loaded on steel side; and (b) S-51: monolithic steel plate.

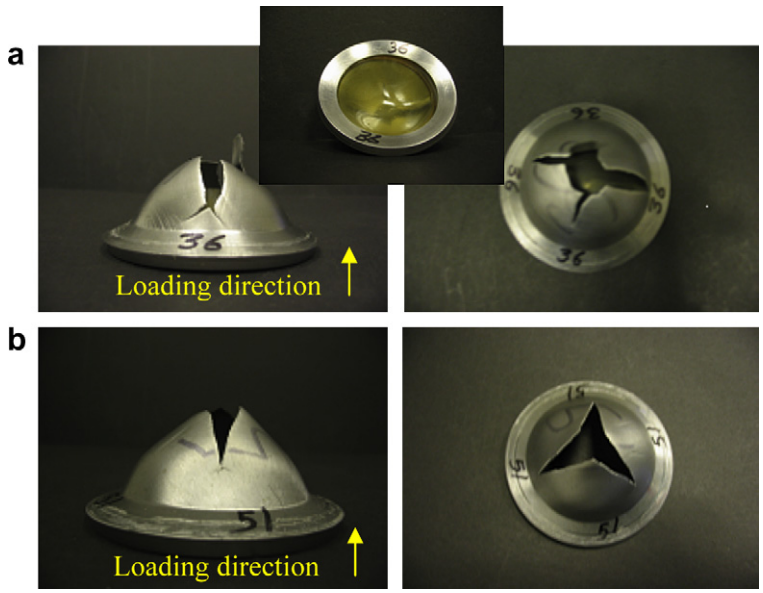

Fig. 8. Deformed steel-plate sample loaded on the dish side at approximately the same kinetic energy per unit thickness: (a) SP-36: bilayer plate loaded on the polyurea side; and (b) S-51: monolithic steel plate.

backed steel plate. Fig. 8 compares two selected plates with the same kinetic energy per unit thickness (approximately 16 kJ/cm) loaded on the dish side (*set-IIB*), one without polyurea coating and the other with polyurea coating on the front side. The steel plate with polyurea failed severely despite having 27.3% more rim rotation compared to the monolithic steel plate.

In addition to the significant shock effect, the polyurea layer has a secondary effect. Provided that the plate does not fail during the initial shock loading, the presence of a polyurea layer, either on the front or on the back face of the steel plate, increases the effective tangent modulus of the plate. Therefore, if the steel plate in a bilayer system does not fail and the polyurea does not detach during the initial shock loading, then the presence of polyurea tends to delay the onset of the necking instability, as has been pointed out by Hutchinson [17]. However, Hutchinson's analysis is mainly under quasi-static conditions, ignoring the influence of the initial shock effect and using a simple constitutive model and geometry.

4. Summary and conclusions

In this article, the dynamic behavior of circular, monolithic steel and bilayer steel–polyurea plates is investigated experimentally using a reverse ballistic experimental setup. This setup allows the application of an impulsive pressure onto a sample, producing severe plastic deformation of the steel plate by extensive stretching and possible fracturing and petaling near the central region of the plate.

Since the membrane stiffness of a thin plate varies linearly with its thickness while its bending stiffness relates linearly to the square of its thickness, the energy absorbed by the specimen's plastic deformation has an essentially linear relation with its thickness under high-velocity impact that produces large stretching deformations. The experiments show that the samples fail when the kinetic energy per unit thickness of the steel plate exceeds an experimentally established critical value which may vary as the experimental conditions are changed.

In the monolithic steel-plate experiments, fracture seems to begin with the onset of necking. Deformation then localizes, giving rise to large local plastic strains within the neck region where cracks initiate and grow circumferentially near the center, and/or radially towards the edge of the plate, the actual crack path being affected by the imperfections and other parameters. Multiple parallel necking patterns can be visually detected in the central region of some of the deformed samples.

When a polyurea layer is cast onto the impact side, its presence may promote failure during the initial shock effect. Under pressure, the stiffness of the polyurea layer increases substantially, attaining a better impedance match with the steel and thereby increasing the energy that is transferred to the plate. On the other hand, when polyurea is cast onto the opposite to the impact side (*back face*), the initial shock loads the steel plate first and then a part of the shock is captured and dissipated by the polyurea layer. Polyurea can also increase the effective tangent modulus of the bilayer and thus delay the onset of the necking instability. Our experimental results are supported by systematic computational simulations of the entire experiment, employing realistic physics-based constitutive models for the steel (DH-36, in the present work) and polyurea, the results of which are reported in a separate article [1].

Acknowledgments

This work has been supported by an ONR (MURI) grant N000140210666 to the University of California, San Diego, under Dr. Roshdy G. Barsoum's research program.

References

[1] Amini MR, Amirkhizi AV, Nemat-Nasser S. Numerical modeling of response of monolithic and bilayer plates to impulsive loads. Int J Impact Eng 2010;37:90–102.
[2] Nurick GN, Martin JB. Deformation of thin plates subjected to impulsive loading – a review, part II: experimental studies. Int J Impact Eng 1989;8(2):171–86.
[3] Radford DD, McShane GJ, Deshpande VS, Fleck NA. The response of clamped plates with metallic foam cores to simulated blast loading. Int J Solids Struct 2006;43:2243–59.
[4] Teeling-Smith RG, Nurick GN. The deformation and tearing of thin circular plates subjected to impulsive loads. Int J Impact Eng 1991;11(1):77–91.
[5] Olson MD, Nurick GN, Fagnan JR. Deformation and rupture of blast loaded square plates-predictions and experiments. Int J Impact Eng 1993;13(2):279–91.
[6] Menkes SB, Opat HJ. Tearing and shear failure in explosively loaded clamped beams. Exp Mech 1973;13:480–6.
[7] Nurick GN, Shave GC. The deformation and tearing of thin square plates subjected to impulsive loads – an experimental study. Int J Impact Eng 1996;18(1):99–116.
[8] Amini MR, Isaacs JB, Nemat-Nasser S. Investigation of effect of polyurea on response of steel plates by direct ballistic experiments. Mech Mater, accepted for publication.
[9] Amini MR, Simon J, Nemat-Nasser S. Numerical modeling of effect of polyurea on response of steel plates to impulsive loads in direct ballistic experiments. Mech Mater, accepted for publication.
[10] Mock W, Balizer E. Penetration protection of steel plates with polyurea layer. In: Presented at polyurea properties and enhancement of structures under dynamic loads, Airlie, VA; 2005.
[11] Nemat-Nasser S, Guo W-G. Thermomechanical response of DH-36 structural steel over a wide range of strain rates and temperatures. Mech Mater 2003;35:1023–47.
[12] The Dow Chemical Company. Isonate® 2143L; modified MDI; 2001. Midland, MI.
[13] Air Products and Chemicals, Inc.. Polyurethane specialty products; 2003. Allentown, PA.
[14] Lee G. Effect of processing temperature on dynamic and thermal properties of Versatane. Unpublished communication. NSWC, Carderock, VA; 2004.
[15] Knauss WG. Viscoelastic material characterization relative to constitutive and failure response of an elastomer. Interim report to the Office of Naval Research. Pasadena, CA: CALTECH; 2003.
[16] Amirkhizi AV, Isaacs J, McGee J, Nemat-Nasser S. An experimentally-based viscoelastic constitutive model for polyurea, including pressure and temperature effects. Phil Mag 2006;86(36):5847–66.
[17] Hutchinson JW. Notes on necking retardation in metal–elastomer bilayers. Personal communication; 2005.